The Chemistry of CO_2 Reduction Processes: Mechanisms, Challenges, and Perspectives

André E. Nogueira, Lucas S. Ribeiro, Jose D. C. Geovo, Francisco N. Souza Neto, Vanessa H. Fragal, Thiago Sequinel, Emerson R. Camargo, and Luiz F. Gorup

Contents

A. E. Nogueira (✉) · J. D. C. Geovo
Department of Chemistry, Institute of Exact and Biological Sciences (ICEB), Federal University of Ouro Preto-UFOP, Ouro Preto, MG, Brazil
e-mail: andre.esteves@ufop.edu.br

L. S. Ribeiro · F. N. Souza Neto · E. R. Camargo
LIEC – Interdisciplinary Laboratory of Electrochemistry and Ceramics, Department of Chemistry, UFSCar-Federal, University of São Carlos, São Carlos, SP, Brazil

V. H. Fragal
Department of Chemistry, UEM – State University of Maringa, PR, Maringá, Brazil

T. Sequinel
Faculty of Exact Sciences and Technology (FACET), Federal University of Grande Dourados, Dourados, MS, Brazil

L. F. Gorup (✉)
School of Chemistry and Food Science, Federal University of Rio Grande, Rio Grande, RS, Brazil

Materials Engineering, Federal University of Pelotas, Pelotas, RS, Brazil

Institute of Chemistry, Federal University of Alfenas, Alfenas, MG, Brazil

R. Gupta, (ed.), *Handbook of Energy Materials*,
https://doi.org/10.1007/978-981-16-4480-1_47-1

Abstract

Anthropogenic CO_2 emissions due to fossil fuels as an energy source have caused an accumulation of this gas in the atmosphere. Consequently, there is a worsening of the greenhouse effect and an increase in the planet's temperature. The need to replace fossil fuels and concerns about energy supply and energy efficiency led to the rise in research on renewable sources as an energy source, such as solar energy. In this context, artificial photosynthesis appears as a solution, allowing the use of renewable sources as a font of energy and the reduction and recycling of waste products, such as CO_2 gas. In this process, the photocatalytic conversion of carbon dioxide into hydrocarbons and other carbon-based materials occurs. Among the products, CO, CH_4, HCOOH, and CH_3OH are produced in higher quantities. This chapter will describe the chemistry underlying the CO_2 reduction, focusing on the electrochemical, photoelectrochemical, and photocatalytic processes. It will also be shown how these methods have contributed to the advancement of CO_2 as a raw material for the synthesis of other compounds with more excellent added value.

Keywords

Artificial photosynthesis · Semiconductors · CO_2 photoreduction · Solar fuels · Thermodynamics

Introduction

High population growth has resulted in exponential increase of energy demand. The use of non-renewable energy sources, such as fossil fuels, has led to a drastic increase in CO_2 emissions in recent decades, accumulating in the atmosphere, thus leaving its cycle unbalanced. Due to this imbalance, the greenhouse effect has intensified, generating several environmental problems, such as the increase in the Earth's average temperature. Other issues such as changes in dissolved CO_2 levels in lakes, rivers, and seas should also be considered, mainly because they promote irreversible changes in marine life as the acidity of seawater increases due to CO_2 dissolution. From 1990 to 2018, CO_2 emissions in the world increased by 152.50.09 $MtCO_2$/year, which corresponds to the rise of 67%, mainly due to the electricity sector (Fig. 1) (Crippa et al. 2019). Thus, there is a need to develop sustainable alternatives for both generation and consumption of energy, using technologies capable of neutralizing the CO_2 balance and generating value for the formed products and even combining environmental, energetic, and financial benefits.

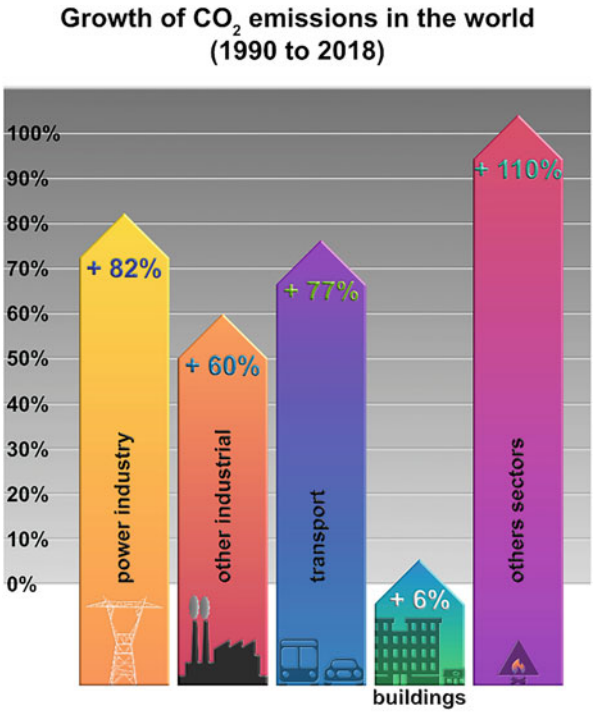

Fig. 1 Growth of CO_2 emissions in the world with amount expressed as a percentage value between 1990–2018. Highlighting the power industry's contribution with the other economy sectors such as other industrial, transport, building, and other sector

One way to reduce CO_2 emissions into the atmosphere is through renewable energy, such as solar and wind. However, these energy sources have severe intermittency or seasonality problems over a day or a year. Therefore, it is necessary to develop technologies that allow the storage of these energy sources. An alternative is to use CO_2 as a raw material to generate other products of interest, such as methane, ethanol, and molecules with longer carbon chains, which can solve the intermittency/seasonality of renewable energy sources through chemical energy storage (Gielen et al. 2016).

This process, which is based on the reduction of CO_2, can be carried out via photochemical or photoelectrochemical reduction. Still, the efficiency of this process is quite limited, which makes its application on an industrial scale impossible. In this scenario, advances in catalytic processes to promote these reactions are essential to convert CO_2 into products with high added value. The conversion of CO_2 into higher added value products is based on the principles of photosynthesis, a mechanism used by plants to convert CO_2 and water into hydrocarbons. This process occurs due to the presence of the chlorophyll B molecule, which acts as a catalyst and, when activated by sunlight, promotes redox reactions (CO_2 reduction and water oxidation) (Fig. 2) (Wang and Domen 2020). Understanding this process is fundamental to comprehend the main methods used in CO_2 conversions, such as the electrocatalytic and photocatalytic routes using heterogeneous catalysts.

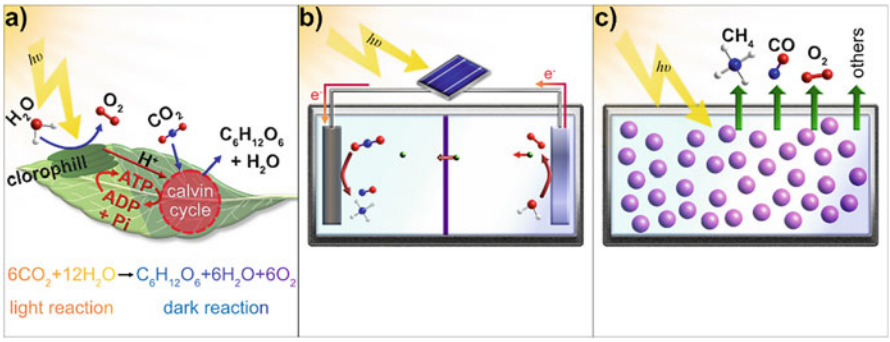

Fig. 2 (**a**) Natural photosynthesis, (**b**) electrochemical synthesis on electrocatalysts powered by a photovoltaic, and (**c**) photochemical synthesis on powdery photocatalysts

Physical and Chemical Aspects of CO_2

Carbon dioxide is a compound of one carbon with the formula CO_2, in which carbon is covalently bonded to each oxygen atom by a double bond. Carbon dioxide is a non-flammable, colorless, odorless, and slightly acidic gas at room temperature and atmospheric pressure. It is produced during respiration by all animals, fungi, and microorganisms that depend directly or indirectly on living or decaying plants for food. It is denser than atmospheric air and highly soluble in water (Table 1), so it can be used as a solvent, vasodilator, anesthetic, refrigerant gas, fire extinguishers, and foam rubber plastics and is one of the leading greenhouse gases (Song 2002).

CO_2 can also produce several products such as ethanol, methanol, methane, and formic acid by different CO_2 reduction processes (Nogueira et al. 2020b). Several research groups have been dedicated to elucidating the various fundamental thermodynamic aspects of the CO_2 reduction process and the reaction mechanisms involved. This description is essential to understand the challenges in this area. Oxidation-reduction reactions involving CO_2 and H_2O to obtain the products mentioned above are endothermic ($\Delta_r H > 0$) and non-spontaneous ($\Delta_r G > 0$), as the reaction to obtain CH_4 has a standard Gibbs energy of +818 kJ mol^{-1} (Table 2) (Ulmer et al. 2019). CO_2 molecule is chemically inert due to its electronic and geometric properties and high thermodynamic stability due to the high energy of the double bond (750 kJ mol^{-1}) (Chang et al. 2016). Even CO_2 reduction reactions are complicated to happen, and their industrial processes require a higher energy expenditure than conventional processes to obtain the same compounds.

Fundamentals of the CO_2 Reduction Process

For CO_2 reduction to occur, it is necessary to provide extra external energy, which can come from a radiation source (photochemical process), by an electrical energy source. An example of applying an electrical potential difference (electrochemical

Table 1 Physical and chemical properties of CO_2. (Song 2002)

Property	Value and unit
Molecular weight	44.01 g/mol
Sublimation point at 1 atm (101.3 kPa)	−78.5 °C
Triple point at 5.1 atm (518 kPa)	−56.5 °C
Critical temperature (T_c)	31.04 °C
Critical pressure (P_c)	72.85 atm (7383 kPa)
Critical density (ρ_c)	0.468 g/cm^3 or 468 g/L
Gas density at 0 °C and 1 atm (101.3 kPa)	1.976 g/L
Liquid density at 0 °C and 1 atm (101.3 kPa) 25 °C and 1 atm CO_2 (101.3 kPa)	928 g/L 0.712 vol/vol
Solid density	1560 g/L
Specific volume at 1 atm and 21 °C	0.546 m^3/kg
Latent heat of vaporization at the triple point (−78.5 °C) at 0 °C	353.4 J/g 231.3 J/g
Viscosity at 25 °C and 1 atm CO_2 (101.3 kPa)	0.015 cP (mPas)
Solubility in water at 0 °C and 1 atm (101.3 kPa) 25 °C and 1 atm (101.3 kPa)	0.3346 g CO_2/100 g-H_2O or 1.713 mL CO_2/mL-H_2O at 0 °C 0.1449 g CO_2/100 g-H_2O or 0.759 mL CO_2/mL-H_2O at 25 °C
Heat of formation at 25 °C	−393.5 kJ/mol
Entropy of formation at 25 °C	213.6 J/Kmol
Gibbs free energy of formation at 25 °C	−394.3 kJ/mol

process) or it can be performed by coupling these two processes in a photo-electrochemical system (Table 3).

In the mentioned processes, CO_2 reduction reactions using heterogeneous catalysts occur in three main stages: (i) adsorption of CO_2 (oxidizing agent) and H_2O (reducing agent), (ii) CO_2 reduction (electron transfer), and (iii) product desorption. In processes that use light as an energy source, there are two more steps in the CO_2 photochemical reduction process: absorption of light/photons to produce electrons ($e-$) and holes ($h+$) and separation of the generated holes and electrons. The steps of adsorption and activation of CO_2 on the active sites generally govern the activity of the process. However, the process selectivity depends on the three stages, i.e., the way the CO_2 is adsorbed, its activation, and the adsorption/desorption energy of its intermediates (Fig. 3) (Chang et al. 2016).

In the heterogeneous photocatalysis process occurs the phenomenon of electron transfer from the valence band (VB) to the conduction band (CB), if semiconductors are illuminated with a visible and UV light source (natural or artificial) with energy equal to or greater than the bandgap energy. In this case, the formation of $e-/h+$ pairs occurs, that is, reducing and oxidizing sites, respectively. These pairs can exhibit internal recombination or migrate to the surface of the semiconductor. On the surface, it can show external recombination or participate in redox reactions with adsorbed species, such as H_2O, H^-, O^2, CO_2, and organic compounds (Ohtani 2010).

Table 2 Reaction pathway of CO_2 reduction and the Gibbs free energy (Grol et al. 2017; Navarro-Jaén et al. 2021)

Reaction pathway	Product	ΔH (kJ/gmol)	ΔG (kJ/gmol)
Hydrogenation reaction (298 K)			
$CO_{2(g)} + H_{2(g)} \rightarrow HCO_{2(g)}$	Formic acid	15.0	43.6
$CO_{2(g)} + 2H_{2(g)} \rightarrow H_2CO_{(g)} + H_2O_{(g)}$	Formaldehyde	35.8	55.9
$CO_{2(g)} + 3H_{2(g)} \rightarrow H_3COH_{(g)} + 2H_2O_{(g)}$	Methyl alcohol	−53.3	−1.0
$CO_{2(g)} + 4H_{2(g)} \rightarrow CH_{4(g)} + 2H_2O_{(g)}$	Methane	−164.9	−113.6
Syngas constituent reactions (298 K)			
$CO_{2(g)} + C_{(s)} \rightarrow 2CO_{(g)}$	Reverse Boudouard	172.5	118.0
$CO_{2(g)} + H_2O_{(g)} \rightarrow O_{2(g)} + H_{2(g)} + CO_{(g)}$	Syngas/oxygen	524.8	485.6
$CO_{2(g)} + CH_{4(g)} \rightarrow 2CO_{(g)} + 2H_{2(g)}$	Dry methane reforming	247.4	170.4
$2H_2O_{(g)} \rightarrow 2H_{2(g)} + O_{2(g)}$	Hydrogen	241.9	158.5
Mineralization reactions (298 K)			
$CaSiO_{3(s)} + CO_{2(g)} \rightarrow CaCO_{3(s)} + SiO_{2(s)}$	Limestone + Silica (1)	−137.48	−91.64
$Ca_2SiO_{4(s)} + 2CO_{2(g)} \rightarrow 2CaCO_{3(s)} + SiO_{2(s)}$	Limestone + Silica (2)	−724.44	−628.69
Photosynthesis (298 K)			
$6CO_2 + 6H_2O \rightarrow C_6H_{12}O_6 + 6O_2$	Glucose	–	2829.4
Photoreduction			
$H_2O \rightarrow H_2 + 1/2O_2$	Hydrogen	–	237.0
$CO_2 \rightarrow CO + 1/2O_2$	Carbon monoxide	–	514.2
$CO_2 + 2H_2O \rightarrow CH_3OH + 3/2O_2$	Ethanol	–	689.0
$CO_2 + 2H_2O \rightarrow CH_4 + 2O_2$	Methane	–	800.0

Table 3 CO_2 transformation technologies. (Kamkeng et al. 2021)

Technology	Type of energy	Temperature	Pressure
Electrochemical	Electricity	Ambient temperature	Ambient pressure
Photochemical	Light	Ambient temperature	Ambient pressure
Photoelectrochemical	Electricity/Light	Ambient temperature	Ambient pressure
Reforming	Heat	600–900 °C	1 bar
Hydrogenation	Hydrogen	200–500 °C	1–100 bar
Carboxylation	Heat	25–350 °C	1–150 bar
Plasma catalysis	Electricity/Light/Heat	25–150 °C	1 bar

The $h+$ generated in the valence band of a semiconductor are efficient oxidizing agents, with a reduction potential between +1.0 and +3.5 V, compared to the standard hydrogen electrode (SHE). On the other hand, the conduction band electrons are good reducers, varying their potential from +0.5 to −1.5 V concerning SHE. These values depend on the electronic band structure of the semiconductors (Fig. 4). In this way, the holes can oxidize the molecules of water adsorbed on the semiconductor surface, generating H^+ (Mao et al. 2013). The photogenerated electrons in the conduction band can react with molecules adsorbed on the surface, such as CO_2,

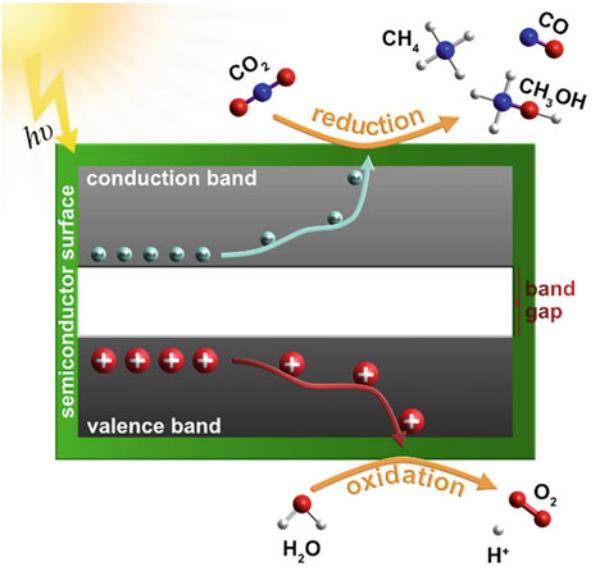

Fig. 3 Diagram of the steps of the CO_2 photoreduction process using a semiconductor

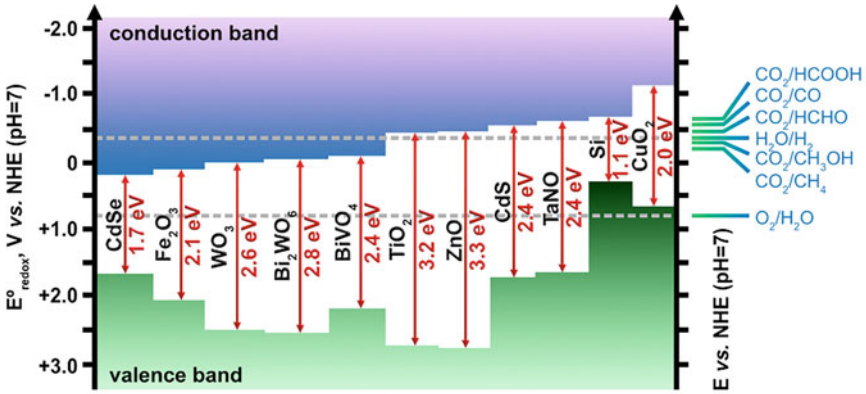

Fig. 4 Band structure of different semiconductors

reducing different carbon monoxide, methane, methanol, and ethanol. In addition to analyzing photocatalysts' structural and optical properties, it is necessary to interpret the potential energy diagrams about the reactions of interest. Figure 4 shows the bandgap energies of some materials and the positions of the respective valence and conduction bands at pH = 7 (Xie et al. 2016).

Each photocatalytic reaction has an energy potential, which varies according to the reaction medium. Table 4 shows the CO_2 reduction reactions and their respective potentials.

Table 4 Electrochemical reactions involved in aqueous CO_2 reduction and proton reduction with corresponding E° reduction potentials (V vs. EPH at pH 7.0). (Jin and Kirk 2016; Sun et al. 2017; da Silva et al. 2021)

Products	Equation	E° (V)[a]
Formic acid	$CO_2 + 2H^+ + 2e^- \rightarrow HCOOH$	−0.610
	$CO_2 + 2H_2O + 2e^- \rightarrow HCOOH^- + OH^-$	−1.491
Carbon monoxide	$CO_2 + 2H^+ + 2e^- \rightarrow CO + H_2O$	−0.530
	$CO_2 + 2H_2O + 2e^- \rightarrow CO + 2OH^-$	−1.347
Formaldehyde	$CO_2 + 4H^+ + 4e^- \rightarrow HCHO + H_2O$	−0.48
Methanol	$CO_2 + 6H^+ + 6e^- \rightarrow CH_3OH + H_2O$	−0.380
	$CO_2 + 5H_2O + 6e^- \rightarrow CH_3OH + 6OH^-$	−1.225
Methane	$CO_2 + 8H^+ + 8e^- \rightarrow CH_4 + 2H_2O$	−0.240
Methane	$CO_2 + 6H_2O + 8e^- \rightarrow CH_4 + 8OH^-$	−1.072
Ethylene	$2CO_2 + 12H^+ + 12e^- \rightarrow C_2H_4 + 4H_2O$	−0.349
Ethylene	$2CO_2 + 8H_2O + 12e^- \rightarrow C_2H_4 + 12OH^-$	−1.177
Ethanol	$2CO_2 + 12H^+ + 12e^- \rightarrow C_2H_5OH + 3H_2O$	−0.329
Ethanol	$2CO_2 + 9H_2O + 12e^- \rightarrow C_2H_5OH + 12OH^-$	−1.157
Ethane	$2CO_2 + 14H^+ + 14e^- \rightarrow C_2H_6 + 4H_2O$	−0.270
Propanol	$3CO_2 + 18H^+ + 18e^- \rightarrow C_3H_7OH + H_2O$	−0.310
	$2CO_2 + 2H^+ + 2e^- \rightarrow H_2C_2O_4$	−0.913
	$2CO_2 + 2e^- \rightarrow C_2O_4^{2-}$	−1.003
	$CO_2 + 2H^+ + 4e^- \rightarrow HCHO + H_2O$	−0.480
	$CO_2 + 3H_2O + 4e^- \rightarrow HCHO + 4OH^-$	−1.311
	$CO_2 + 4H^+ + 4e^- \rightarrow C + 2H_2O$	−0.200
	$CO_2 + 2H_2O + 4e^- \rightarrow C + 4OH^-$	−1.040
Methanol	$\frac{4}{3}HCO_3^- + \frac{28}{3}H^+ + 8e^- \rightarrow \frac{4}{3}CH_3OH + \frac{8}{3}H_2O$	−0.374
Acetate	$2HCO_3^- + 9H^+ + 8e^- \rightarrow CH_3COO^- + 4H_2O$	−0.285
Methane	$HCO_3^- + 9H^+ + 8e^- \rightarrow CH_{4(aq)} + 3H_2O$	−0.259

[a]Theoretical CO_2 reduction potentials are given relative to the SHE at pH 7.0 and room temperature in water

Analyzing the diagram in Fig. 4 and Table 4, it can be seen, for example, that Cu_2O is a material that can be used in almost all reactions since its valence and conduction bands encompass all the energy potentials of the responses studied at this pH. In the case of the CO_2/CH_4 reaction, a suitable photocatalyst would be TiO_2. Fe_2O_3 or CdSe is used as a photocatalyst; the absence of CH_4 is justified by the lower position of the conduction band about the redox potential of the reduction reaction of CO_2 in CH_4.

Another way to convert CO_2 into other products is through a photoelectrochemical cell system (PEC), in which photoelectrocatalysis can be defined as an extension of photocatalysis techniques. Photoelectrocatalysis is the application of a potential to the photocatalytic process. The applied potential optimizes the efficiency of photocatalysis, as it minimizes the recombination of the photogenerated $e-/h+$ pair and increases the transfer rate of electrons and holes to their respective

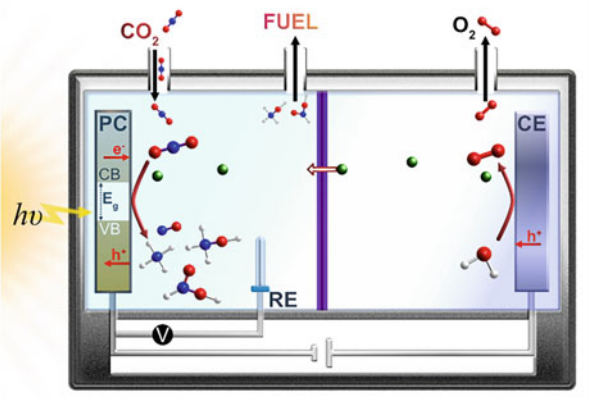

Fig. 5 A photoelectrochemical cell with a photocathode (PC) for CO_2 reduction, a counter-electrode (CE) for water oxidation, and a reference electrode (RE)

acceptors. The action of light allows the potential or current applied in the reaction to be smaller than those used in electrocatalysis (Kumaravel et al. 2020).

The photoelectrochemical system, in general, is composed of a semiconductor photoelectrode (work electrode), a counter-electrode (CE), and generally a reference electrode (RE) (Fig. 5). The semiconductor photoelectrode is activated with UV or visible radiation, generating charge carriers. The reduction of CO_2 in the photoanode and the oxidation of water in the counter-electrode will occur. In this way, the redox reaction products can be spatially separated by a membrane, which can exclude the possibility of reoxidation of the CO_2 reduction products (Kumaravel et al. 2020).

Furthermore, compared to the photocatalytic system, the PEC system can achieve greater efficiency since an external polarization can promote the efficient separation of the photogenerated $e-/h+$ pairs, decreasing their recombination rate.

Adsorption

As mentioned before, the CO_2 photoreduction process takes place in different steps that involve adsorption, activation, and dissociation of the C-O bond. Activating this molecule is one of the biggest challenges, as CO_2 is highly stable and inert. Furthermore, competition with other possible reduction reactions – notably, the evolution of H_2 by photolysis of water and the reduction of O_2 to $O_2^{\bullet}$ – significantly reduces the efficiency of this reaction of interest. Thus, understanding the interaction of the CO_2 molecule with the semiconductor surface is essential to increase both the activity of photocatalysts and the selectivity of the products generated in the process.

The interaction of the CO_2 molecule with the surface of the material leads to the formation of partially charged species $CO_2^{\delta-}$ through interactions with surface atoms (Fig. 6). The CO_2 molecule has a linear structure, in which each of the oxygen atoms has a single pair of electrons that can be donated to Lewis acid sites present on the surface of the catalysts (Fig. 6a). On the other hand, if the materials have Lewis acid

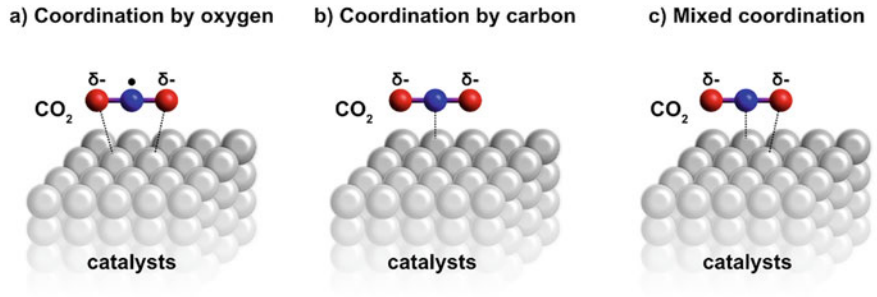

Fig. 6 Representative scheme of possible adsorbed CO_2 species on the surface of a catalyst

sites, the carbon atom of the CO_2 molecule can receive these electrons forming carbonate-like species (Fig. 6b) (Dzade 2020). Furthermore, suppose the material has both basic and acid sites, acting simultaneously as an electron donor and acceptor. In that case, mixed coordination with the CO_2 molecule can be formed, as shown in Fig. 6c.

Thus, primary Lewis sites in catalysts can adsorb and activate CO_2, while Lewis acid sites can promote the dissociation of H_2O. The dissociation of the H_2O molecule, as already mentioned, also affects yield and selectivity, and therefore, essential and acid sites are considered equally important in the CO_2 photoreduction process. In this way, the acid-base properties of the materials, which include type (Bronsted acid/base [proton donors/acceptors] vs. Lewis acid/base [electron donors/acceptors]), strength, concentration, and location, are characteristics that directly affect activity and selectivity during catalytic reactions (Sakhno et al. 2010; Diallo-Garcia et al. 2014; Chong et al. 2018).

Zhenyu Sun and collaborators showed that the formation of formate ($HCOO^-$) and formic acid (HCOOH) from the reduction of CO_2 using electrocatalysis could occur by several mechanisms that involve different types of interaction of the CO_2 molecule with the electrode surface (Fig. 7) (Sun et al. 2017). The first mechanism of formic acid (HCOOH) formation can occur through the interaction of one oxygen atom (monodentate) or two oxygen atoms (bidentate) of the CO_2 molecule with the electrode surface (Fig. 7a). Another alternative is through the formation of adsorbed $CO_2^{\bullet -}$ radicals react with neighboring water or proton to generate $HCOO^-$ or HCOOH. In addition, the CO_2 molecule can be adsorbed on the surface of the material, forming carbonate, which undergoes transfers of two electrons and a proton to form $HCOO^-$ which is desorbed (Kortlever et al. 2015).

Influence of pH

An important parameter that must be taken into account in the CO_2 reduction process is the pH of the solution, as the pH affects several factors, such as the concentration of dissolved CO_2, the potential for reduction reactions, the availability of protons, the stability of semiconductors, and the species of carbon dissolved in the reaction

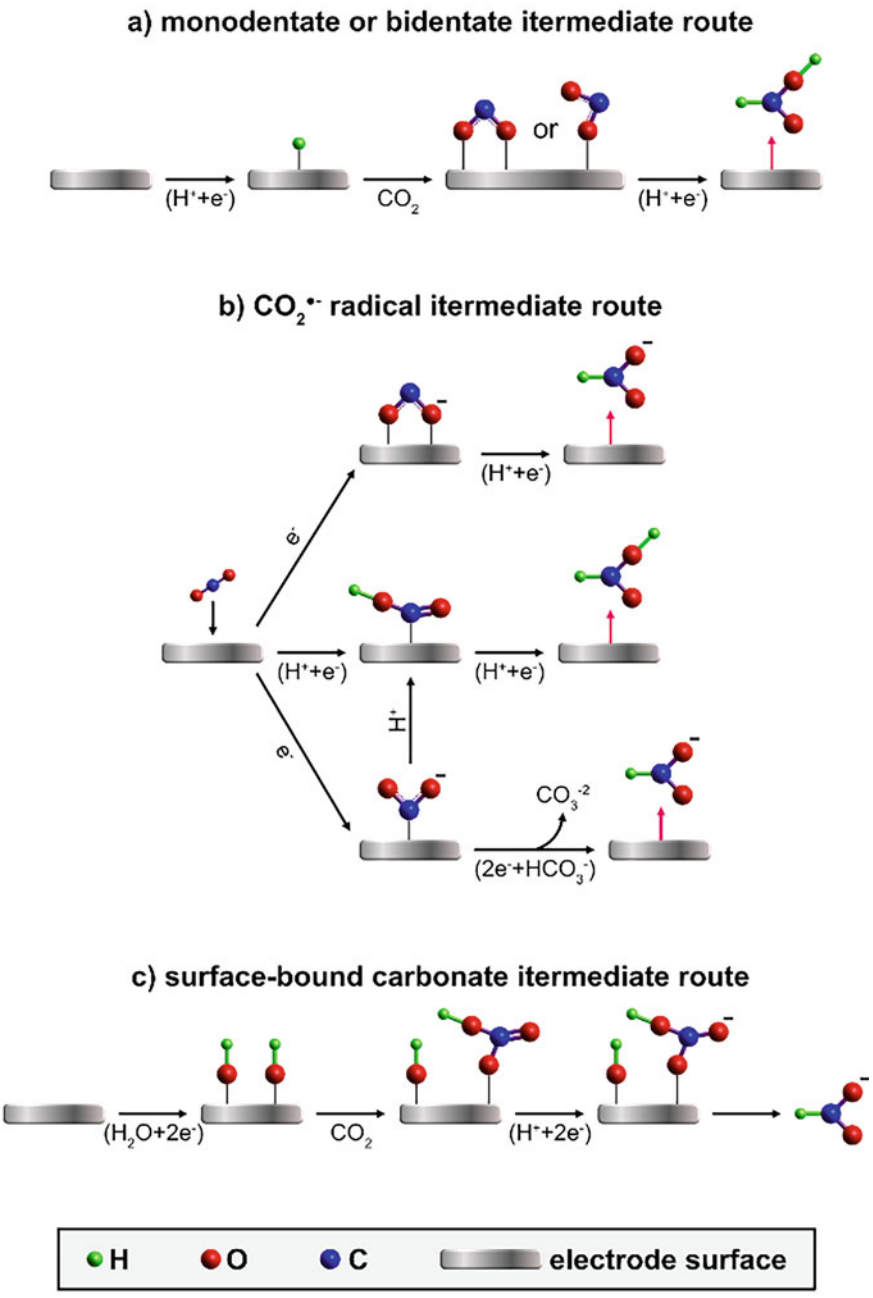

Fig. 7 Possible reaction pathways for the electrocatalytic reduction of CO_2 to $HCOO^-$ or HCOOH

medium. Figure 8 shows how the carbon species vary according to the pH of the reaction medium, where it can be seen that at pH $\leq$ 5.0, the predominant species is H_2CO_3, at pH $\geq$ 12 the species CO_3^{2-}, and at 6.0 $\leq$ pH $\leq$ 11.0 the HCO_3^- species predominates despite having the other ions in a smaller percentage in equilibrium (Liu et al. 2021). The species present in the reaction medium modify both the reduction potential and the interaction capacity of these species with the surface of the materials caused by the modification of the point charge-zero (PCZ) of the surface of the materials.

In addition to the different reduction potential of carbon species, the prospects of CO_2 photoreduction reactions at different pH values change to a more negative potential level with increasing pH. In this case, the electrons are photoexcited at a possible level more negative than CO_2 reduction can provide the driving force to reduce CO_2 to the expected chemical reaction (Liu et al. 2021). Thus, choosing the ideal pH about the properties of the semiconductor used is essential to optimize the activity and selectivity of the CO_2 photoreduction process.

Photoreduction of CO_2

Stimulated by the development of new methods for synthesizing and modifying heterogeneous catalysts and the advances obtained both in the degradation process of organic pollutants and in the generation of H_2 via photocatalysis, research on CO_2

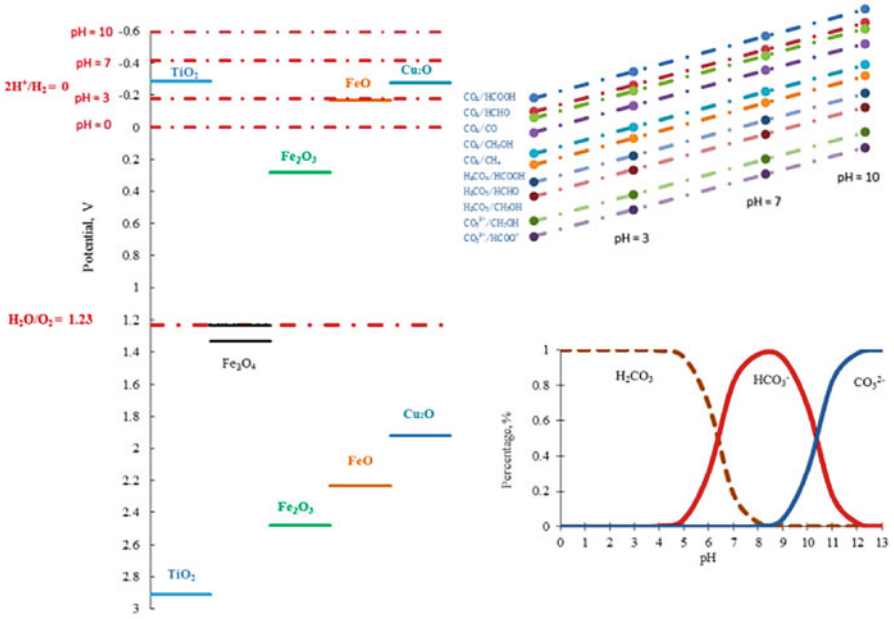

Fig. 8 The potential level of photocatalysts and thermodynamic potential versus pH for CO_2 photoreduction products and hydrogen evolution. (Reproduced with permission from (Liu et al. 2021). Copyright 2021 Chem, Elsevier)

photoreduction is developing rapidly. As in the traditional photocatalytic methods described by Honda and Fujishima in 1972, the CO_2 photoreduction process was demonstrated using semiconductors such as TiO_2 and ZnO for the first time. Even today, these materials are used as a starting point for developing more complex photocatalysts with specific properties that increase the activity of these catalysts in the photocatalytic processes.

Many of the studies on the conversion of CO_2 use heterogeneous catalysts, primarily semiconductors, alone or coupled to other materials. These catalyst semiconductors mostly have a bandgap in the UV region, allowing solar energy as an energy source for the process (White et al. 2015). Since the study of photoelectrochemical reduction of CO_2 using TiO_2 by Inoue et al. in 1979 (Inoue et al. 1979), several semiconductors, both transition metal oxides and carbon-based materials, were used to activate CO_2. The oxides and TiO_2 materials based on ZnO, Nb_2O_5, WO_3, and CuO presented a great capacity to reduce CO_2 in hydrocarbons. Among the carbon-based materials, graphene and graphene oxide stood out (Neațu et al. 2014). This topic will discuss the efficiency and selectivity of these semiconductors in the carbon dioxide photoreduction process.

Titanium Dioxide

Titanium dioxide is widely used as a photocatalyst for CO_2 reduction due to its low toxicity, high durability, and abundance, in addition to appropriate band-edge positions for this process. Kar et al. used TiO_2 to photo reduce CO_2 into hydrocarbons. To improve the activity of the photocatalyst in visible light, the flame annealing technique was used (Kar et al. 2019). As a result, an enhanced CH_4 yield was achieved using flame annealed TiO_2 nanotubes. Furthermore, with isotopes, it was possible to identify that methane was being formed from the carbon dioxide used as a reagent and that the photoreduction process occurred through the carbene pathway. The semiconductor synthesized in this work generated 156.5 μmol/g catalysts.hr. of CH_4, one of the highest values ever reported compared to another works using TiO_2. This high performance is because the material is also active under visible radiation and a square morphology and pure crystalline phase of rutile.

In another study, Wu et al. doped titanium dioxide nanosheets with boron and nitrogen (BNT) using ammonia borane, a green substitute for harmful reagents used to create surface defects TiO_2 (Wu et al. 2021). This doping made Lewis acid-base pairs, rich oxygen vacancies, and a mesoporous structure due to the evolution of H_2. The BNTs synthesized with different amounts of borane ammonia produced a more significant CO than pure material. Then, it was suggested that Lewis acid-base pairs increase the activation of CO_2, facilitating its reduction.

Torres et al. reported the effect of MgO basicity on the photoactivity of nanocomposites formed by MgO and TiO_2 (Torres et al. 2020). TiO_2 nanoparticles were decorated with MgO through physical mixing. The nanocomposites showed more excellent selectivity for CO, with smaller amounts of CH_4, HCCOH, and CH_3COOH also being produced. Except in the case of the material with 1% MgO, a more significant part of the other compounds was made, decreasing the selectivity for

CO. The results also showed that the beneficial effect of MgO occurs only in small quantities since, in larger doses, it starts to have an insulating behavior, reducing photoreduction.

Zinc Oxide

Zinc oxide (ZnO) is also widely used as a photocatalyst due to its low cost, environmental benignness, and good performance. Li et al. synthesized two different types of porous ZnO nanocatalysts varying the exposed facet, (110) and (001) (Li et al. 2020). CO_2 photoreduction tests showed that the material with the (110) characteristic exposed exhibited better photocatalytic activity due to the synergic effects of high charge-separation efficiency, good CO_2 adsorption ability, and better activation of CO_2. Both materials showed high selectivity for CO production, with low amounts of CH_4 also present. Furthermore, the use of the Na_2SO_3 reagent practically doubled the CO production.

Hegazy et al. also applied pure ZnO photocatalysts to photoreduce CO_2 (Hegazy et al. 2020). The materials were prepared at different temperatures (300, 350, and 400 °C), and all presented oxygen vacancies. In the case of material treated at 350 °C, the highest production of methanol, the primary product in UV light, occurred when combined with $NaHCO_3$. It is also, in this case, the highest yield obtained in all tests. For materials treated at 300 and 400 °C, the best reagents were NaCl and NaOH, respectively. Furthermore, the oxygen vacancies in the structure acted in the process, facilitating the charge transfer instead of working as recombination sites, improving the catalytic activity.

Also, it is possible to apply ZnO modified with other materials. Li et al. synthesized photocatalysts by changing ZnO nanorods with In_2O_3 and MoS_2 (Li et al. 2021). The addition of these compounds on the ZnO surface improved the absorption capacity in the visible region. It generated more transfer channels and surface-bound active sites for the photogenerated holes and electrons formed by the surface-bound species. Thus, there was a better separation of the charge carriers. Also, the addition of the two oxides made the ZnO bandgap closer to the redox potential of the CO_2 photoreduction, increasing the amount of CO, the intermediate product, and CH_4, the final product, produced. The yield of CO and CH_4 was higher for the material ZnO-$In_2O_3$3%/MoS_2 2% compared to the three oxides alone.

Niobium Oxide

Niobium pentoxide Nb_2O_5 is a semiconductor that has catalytic activity due to the acidity of its surface. Additionally, it has a photocatalytic activity for the degradation of pollutants. da Silva et al. were the first to demonstrate the catalytic activity of Nb_2O_5 in the photoreduction of CO_2 (da Silva et al. 2019). The catalysts were prepared by the oxidizing peroxo method (OPM) and different annealing

temperatures. The results showed that all materials presented activity for the photoreduction of CO_2 and that the higher the treatment temperature, the lower the acidity of the material (Nogueira et al. 2018). Besides, activity and selectivity were shown to be related to surface acidity. A high edge favored the production of CO, HCOOH, and CH_3COOH, while a low acidity favored the formation of CH_4. It was also shown that CO is the central intermediate for producing the other compounds.

Oliveira et al. also used catalysts based on Nb_2O_5, synthesizing nanocomposites with basic bismuth nitrates (BBN/Nb_2O_5) (Oliveira et al. 2021). Two different temperatures were used in the hydrothermal synthesis, 120 and 230 °C. The results showed that the first temperature maintained the BBN precursor's crystal lattice, and the materials proved to be active for CO_2 reduction. The main products were CO and CH_4, in smaller quantities. On the other hand, the materials synthesized at 230 °C presented a lamellar structure of $Bi_2O_2(OH)(NO_3)$ and a bandgap that prevented the reduction of CO_2. Furthermore, photoreduction tests showed that BBN material alone is not capable of producing CH_4, only together with Nb_2O_5. Even CH_4 production using Nb_2O_5 also increases with the presence of BBN. The scavenger experiments showed that photoreduction occurs by a mechanism based on a Z-scheme with the molecules being oxidized in the valence band of Nb_2O_5 and CO_2 being reduced in the conduction band of BBN.

In another study of catalysts based on Nb_2O_5, Nogueira et al. observed that the addition of 2.5% CuO increased the efficiency of the photoreduction process and the selectivity for the production of CH_3COOH concerning pure Nb_2O_5 (Nogueira et al. 2020a). However, increasing the percentage of CuO resulted in an increase in selectivity for CH_4. Furthermore, the CO molecule was proven to be an intermediate for the production of CH_3COOH.

Tungsten Oxide

Another oxide semiconductor used in artificial photosynthesis is tungsten oxide. Oxygen-deficient WO_3 can absorb both UV-vis and NIR radiation, as well as release trapped electrons. Liang et al. performed CO_2 reduction using synthetic ultrathin cubic-WO_3 layers without using a sacrificial reagent and employing IR radiation (Liang et al. 2018). Theoretical calculations showed that oxygen vacancies from a critical density value create an intermediate band. Due to this property, the synthesized material could absorb NIR radiation and split the CO_2 molecule into CO and O_2. Moreover, the semiconductor maintained its activity without reduction even after nine cycles in 3 days of testing.

Zhu et al. also studied the application of WO_3 semiconductors to reduce CO_2 in higher value-added molecules (Zhu et al. 2018). Using a hydrothermal sol-gel route, Pd-Au/TiO_2-WO_3 nanoparticles were prepared. The photoreduction tests showed that the best composition was with 0.5%wt of Pd and 0.1%wt of Au. In this case, the production rates of CO and CH_4 were, respectively, 271.3 μmol g^{-1} h^{-1} and 39.1 μmol g^{-1} h^{-1}. Compared with the pure TiO_2 catalyst, the production of CO was 247 times higher and of CH_4 43 times higher. The authors believe that this better

performance is related to the increased surface area and the low recombination rate of photogenerated electron-hole pairs.

Another way to apply tungsten oxide is in conjunction with molybdenum oxide. Liu et al. synthesized a photocatalyst formed by the heterojunction of WO_{3-x}/MoO_{3-x} by the solvothermal process (Liu et al. 2021). In this methodology, WO_{3-x} nanowires were grown on MoO_{3-x} nanosheets. The characterization showed that the resulting material presents oxygen vacancies, besides promoting the separation of electron-hole pairs. These properties, together with an improvement in surface area, allow this semiconductor to give enhanced CO_2 adsorption and activation, in addition to more excellent photoreduction activity. The CO and CH_4 production yields compared to the pure MoO_{3-x} photocatalyst were, respectively, 9.5 and 8.2 higher.

Copper Oxide

Copper oxides are among the most promising semiconductors for photoreducing CO_2. However, its instability is still a big problem for its use. An example is CuO, which can be used pure or conjugated with another material as a composite or heterojunction. Nogueira et al. studied the role of CuO in the CO_2 photoreduction process. Photoreduction tests have shown that this oxide acts as a reactant during reduction through the formation of copper carbonate (Nogueira et al. 2020b). However, this malachite formed ($Cu_2(OH)_2CO_3$) acts as a catalyst, helping to produce hydrocarbons. During the conversion of oxide to copper malachite, there is a significant conversion of CO_2 to CH_4, which decreases with complete carbonate formation. In addition, the authors also observed that the electrolyte used interferes with the product's selectivity. The use of NaOH led to the production of CH_4, while the use of $Na_2C_2O_4$ produced CO, and $KBrO_3$ primarily generated O_2 (Nogueira et al. 2019).

Ribeiro et al. studied the activity of another copper oxide as a photocatalyst for artificial photosynthesis. $CuBi_2O_4$ semiconductors were synthesized using a microwave-assisted hydrothermal method, resulting in crystalline materials with controlled morphology (Ribeiro et al. 2020). The advantages of this methodology are the low temperature used and the processing time. As for the photoreduction process, the semiconductor showed high selectivity for the production of CH_4, with approximately 90% conversion.

Handoko et al. also employed copper oxide as a photocatalyst (Handoko and Tang 2013). In this study, the semiconductor CuO, with different facets exposed, was used in water splitting and CO_2 photoreduction processes. It was observed that the low-index characteristics exhibited more excellent activity for CO_2 photoreduction than the high index facets. Furthermore, it was shown that it is possible to improve the efficiency of the conversion of CO_2 to CO by preparing a heterojunction of Cu_2O with RuO_x. This combination slows down fast charge recombination, in addition to better stabilizing copper oxide. However, in percentages greater than 0.25% wt of RuO_x, the light-blocking effect of ruthenium oxide occurs, decreasing its activity.

Graphene

Carbon-based semiconductors, such as graphene and carbon nitride, have the advantage of being eco-friendly, a high number of active sites, and good thermal and chemical properties. In addition, these materials feature low energy consumption and high surface area regeneration capability. These characteristics make them excellent options as photocatalysts for CO_2 photoreduction. In most cases, semiconductors based on C_3N_4 use ultraviolet radiation, while graphene can use the entire spectrum (Aggarwal et al. 2021).

These carbon semiconductors can be applied together with oxides forming nanocomposites with optimized properties. Olowoyo et al. assembled TiO_2 nanoparticles on reduced graphene oxide (RGO) surface (Olowoyo et al. 2019). The nanocomposite showed high activity in converting CO_2 to methanol in both ultraviolet and visible radiation, indicating better separation of photogenerated carriers. The study also showed that the reaction under UV radiation occurs via the traditional mechanism of photogenerated electron transfer to RGO. However, the mechanism is different in the reaction under visible radiation, with electrons being produced in the RGO and holes in the TiO_2.

Liu et al. decorated RGO with cuprous oxide (Cu_2O) with different morphologies (cubic, octahedral, and rhombic dodecahedral) (Liu et al. 2019). Among the materials, the Cu_2O/RGO crystal with rhombic dodecahedral structure showed the best activity in the CO_2 photoreduction process under visible radiation, surpassing other synthesized semiconductors by 80 times. This superior performance is related to the copper oxide structure used, which allowed a decrease in the energy barrier to transfer photogenerated electrons to the surface. Furthermore, the presence of RGO aided in the transfer of photogenerated electrons from the conduction band of Cu_2O. Karachi et al. evaluated the activity of an RGO-based photocatalyst decorated with Rh_2O_3/Rh nanoparticles (Karachi et al. 2018). The photoreduction tests showed that the number of nanoparticles with the best methane production was 18% wt. In the photoreduction process, the photoinduced electron transfer from the nanoparticles to the graphene sheet occurs, increasing the activity of the nanocomposite. The authors also showed that it is necessary to use a temperature of 175 °C to desorb water molecules formed on the surface of the semiconductor since they deactivate it.

Carbon Nitride

As with graphene, graphitic carbon nitride (g-C_3N_4) can be applied as a heterojunction with an oxide semiconductor. Martins et al. synthesized ZnO heterostructures with g-C_3N_4 varying the latter amount (15%, 50%, and 85%) (de Jesus Martins et al. 2021). The ZnO nanoparticles were prepared by precipitation of zinc oxide in an alkaline solution on the surface of g-C_3N_4. The results showed good interaction between the materials, which led to more excellent stabilization of the semiconductor and, consequently, better separation of photogenerated charge

carriers (Gorup et al. 2020). Among the materials obtained, ZnO:g-$C_3N_4$50% was the highest activity for the photoreduction of CO_2 into CO. In the case of methane production, the material with 15% g-C_3N_4 performed a little better than the others.

Another way to improve the activity of carbon nitride in the CO_2 photoreduction is through its exfoliation to produce carbon nitride nanosheets (CNNS). Inactivity is due to longer photogenerated charge lifetimes and greater surface area. Qin et al. synthesized ultrathin nanosheet g-C_3N_4 using the calcination method (Qin et al. 2021). This material was then compared with the bulk counterpart (B-g-C_3N_4) in the photoreduction of CO_2 to CO under visible radiation. The results showed an almost six times higher CO production using CNNS, the only product. In the case of bulk material, methane and methanol were also produced. This higher activity can be explained by the ultrafine structure (10 nm) and the large number of surface defects that improve the material's ability to adsorb visible light, favoring the transfer of photogenerated carriers. Furthermore, blemishes on the surface alter the way the CO_2 molecule adsorbs on the photocatalyst, changing the selectivity of the products. In the case of NS-g-C_3N_4, the adsorption mode is N-O-C=O, favoring the production of CO. In a bulk material, adsorption occurs differently than N-CO_2, allowing the formation of other products.

Crake et al. also used CNNS for the photoreduction of CO_2 (Crake et al. 2019). However, carbon nitride nanocomposites with titanium dioxide were produced using the hydrothermal method. CNNS was used to control the TiO_2 facet formation. Catalytic tests showed that the nanocomposite has a greater adsorption capacity and activity than the two different materials. It was possible to produce CO using hydrogen gas and water vapor as the sacrificial agent. This increased activity can be explained by forming an artificial photocatalytic Z-scheme. Furthermore, the material with more facets (001) showed more significant activity for photoreduction, as expected.

Photoelectrochemical Process of CO_2 Reduction

The reduction of CO_2 is not a spontaneous reaction; thus, it is necessary to supply energy for this to occur, such as the use of electric current or UV or visible radiation. The use of electric current to force a non-spontaneous chemical reaction is called electrolysis. Electrolysis is carried out with electrodes immobilized in an aqueous medium, with the presence of two electrodes (anode and cathode) connected to an energy source that allows their polarization, making them electrically charged. Reduction reactions occur at the cathode, which is negatively charged and therefore supplies electrons to the compounds to be reduced. Likewise, the anode is positively charged, receiving electrons from compounds that come in contact with it, oxidizing them. Applying a specific electric potential to the electrodes, the oxidation of water at the anode is obtained to form O_2, protons (H^+), and electrons (e^-). At the same time, the electrochemical reduction of CO_2 at the cathode leads to the formation of several products such as carbon monoxide, formic acid, methanol, methane, ethylene, and ethane, as shown in Table 4 (da Silva et al. 2021).

Although this process can convert CO_2 into fuels by renewable means, some performance problems prevent its implementation at an industrial level, such as low energy efficiency, which is expressed in the form of high overpotential, measured in the form of faradic efficiency. For each reaction, a standard potential (E°) describes the thermodynamic equilibrium potential and the free energy required for the reaction to occur. Thus, overvoltage is understood as the difference between the potential that needs to be applied and the thermodynamic equilibrium potential, which can be interpreted as a measure of the activation energy of a given reaction (Ding et al. 2021). Thus, the use of the photoelectrochemical process can help in energy balance.

The photoelectrochemical reduction of CO_2 is performed in a photoelectrochemical cell, which integrates the constituents of a typical electrochemical cell, except the anode and cathode, which have the same function as conventional electrodes but have a different operating mechanism. These photoelectrodes are semiconductors that, when exposed to sunlight, generate excited electrons that are used in the redox reactions of the electrochemical process, reducing the amount of electrical energy needed to force the reduction of CO_2 (non-spontaneous reaction) or the oxidation of H_2O. The type of material that makes up these electrodes depends on the configuration chosen for the photoelectrochemical cell, which can occur by using photocathode and conventional anode (Fig. 9a), photoanode and conventional cathode (Fig. 9b), or photoanode and photocathode (Fig. 9c). (Zhang et al. 2018).

For photoelectrodes to perform their function, they must have a bandgap smaller than 2.2 eV, allowing the electrons to be excited by the absorption of photons from sunlight. However, these holes have to be greater than 1.3 eV so that the generated electrons have enough energy to force the redox reactions of the process. In addition, it is also relevant that these photoelectrodes are stable to corrosion caused by electrolytes. In the case of photocathodes, they have a particle size that allows their catalytic activity, creating active centers that promote the adsorption of the CO_2 on its surface and providing its activation.

In photocathode and photoanode, the most studied materials are the p-type semiconductors, which have an adequate conduction band for the reduction of CO_2. However, these semiconductors have insufficient valence band potential to oxidize water, leading to applying high overpotential.

The scenario is more promising for the system consisting of a photoanode and a conventional cathode since the catalytic activity depends only on the cathode, which is already more developed to produce certain compounds. Thus, the efficiency of the photoanode is determined only by its action, which is evaluated according to its ability to generate protons and electrons by the oxidation of water, as well as to provide a negative potential to the cathode, caused by the incidence of light, which allows reducing the amount of external electrical energy used. Photoanodes are usually composed of n-type semiconductors such as TiO_2, CuO, ZnO, WO_3, and $BiVO_4$, inexpensive, abundant, and potentially corrosion-stable materials (Gorup et al. 2020).

The presence of electrodes that perform the function of catalysts (electrocatalysts) has a fundamental importance in solving the problems described above, promoting

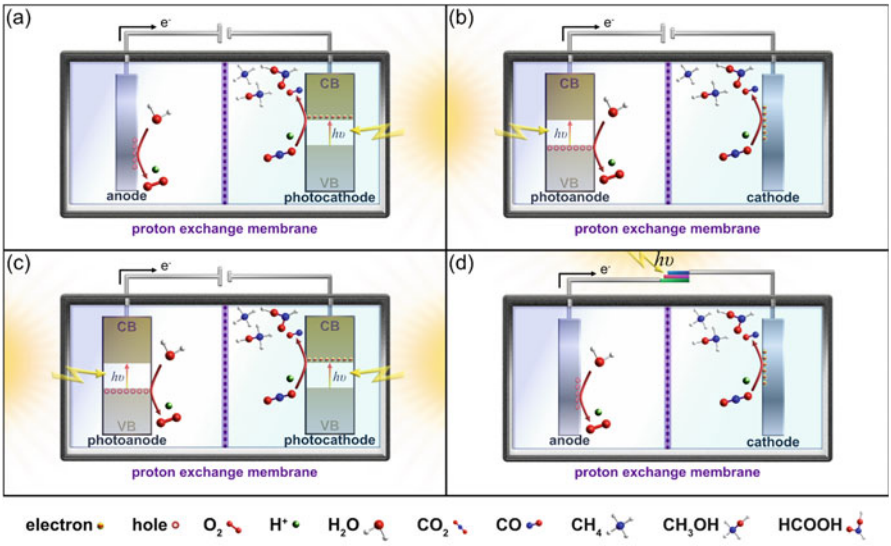

Fig. 9 Schematic diagrams for a photoelectrochemical cell using semiconductors as (**a**) photocathode, (**b**) photoanode, and (**c**) both photoanode and photocathode. (**d**) The schematic diagram for the device combines a photovoltaic cell with an efficient electrochemical catalyst for CO_2 reduction

the optimization of the process in several fields. The most used electrocatalysts in the electrochemical reduction of CO_2 can be classified into the following groups: metals, metallic complexes, non-metallic catalysts, and biocatalysts, which differ according to their composition and morphology.

Challenges and Perspectives

Fossil fuels will still be a significant energy source for the next few decades, which has consequences like increasing CO_2 concentrations in the atmosphere. The adoption of large-scale carbon-negative technologies is necessary to reduce the effects caused by waste CO_2 emission. Despite growing efforts to drastically cut CO_2 emissions and address climate change, energy outlooks project that the world will continue to rely on fossil fuels.

The carbon price also stimulates clean technology and market innovation, fueling new, low-carbon drivers of economic growth as a means of bringing down emissions and driving investment into cleaner options. Recycling CO_2 into fuels, materials, and valuable chemicals has emerged as an opportunity to reduce carbon dioxide emissions for mitigates the effects of global climate change. In this way, CO_2 recycling has a promising potential in the circular carbon economy that can support a net-zero future. However, CO_2 recycling processes have remained costly and difficult to deploy, underscoring the need for government support and RD&D.

Coupling the photocatalytic and electrochemical process for CO_2 reduction using a renewable energy source like solar radiation to convert CO_2 into different organic molecules with higher energy value is a promising strategy to help achieve a sustainable global energy economy. This could not only serve as a CO_2 abatement in the atmosphere, but it is also a way of converting solar energy into chemical energy, making it possible to use the infrastructure currently used for fossil fuels.

The critical challenges to reducing the costs of the CO_2 reduction process are not based solely on a greater fundamental understanding of the mechanism of reduction of the CO_2 molecule, but a general understanding of the factors that influence the activity and selectivity of the products generated, such as voltages applied, the intensity of the radiation, the type of electrolyte, and the properties of the semiconductors used as a photoelectrode. Low photoelectrode stability, proper photoreactor design, and low process selectivity are critical steps for large-scale process implementation. There is still a lot of work to be done in optimizing the photoelectrochemical process before implementing this CO_2 reduction technology on an industrial scale, but it presents itself as a promising technology that will contribute to the advancement of the use of CO_2 as a raw material for synthesis of other compounds with higher added value.

While many challenges and opportunities remain in developing catalysts and reactor systems with high activity, selectivity, stability, and scalability, much progress has also been attained in recent years, priming this technology for commercial application. With continued research and development, electrochemical CO_2 reduction could have a substantial impact on the sustainability of our global energy economy.

In addition, during the United Nations climate conference (COP26), which took place with experts and world leaders, it was detected that more ambitious advances are needed in the coming years to contain CO_2 emissions and, consequently, global warming. In terms of commitments to reduce carbon emissions, India, one of the largest markets in the world, made one of the most ambitious announcements pledging to generate half of the country's electricity from renewable sources by 2030 and reach zero by 2070. In this way, these government efforts are being identified as opportunities to build markets for CO_2 abatement and consequently allow technologies to mature in the coming decades with support and investments in different sectors where CO_2-derived products can play an important role in reducing CO_2 emissions.

The conjunction with RD&D for CO_2 capture from biomass and the air, supported for international RD&D programs and knowledge transfer networks, can facilitate accelerated development and uptake of these technologies. Governments are providing direct funding to demonstrate technologies with good prospects in terms of scalability, competitiveness, and CO_2 emissions reductions; these financial investments are required to stimulate clean technology and market innovation. The CO_2 recycling pathways show real promise for displacing existing fossil fuels intensive production pathways of high-volume products. If implemented globally, these CO_2 recycling pathways (excluding costly methane) could collectively result

in carbon reduction. Finally, a well-crafted innovation policy combined with market-alignment policies can contribute substantially to CO_2 recycling pathways.

Conclusion

We have examined in this chapter the chemistry underlying the CO_2 reduction will be described, focusing on the electrochemical, photoelectrochemical, and photocatalytic processes. It is important to emphasize that many variables continue to be elucidated in the photocatalytic process, which will require a sustained effort over many years. However, there is a stimulating potential for significant improvements in the field of CO_2 photoreduction, mainly in the development of new heterogeneous photocatalysts in which there are still important issues that need to be faced and addressed for a possible scaling of the process, such as (i) how to use the catalyst, (ii) excellent use of solar radiation, and (iii) selectivity of the products formed. However, from the synthesis of heterogeneous catalysts, it remains a challenge to carry out the mass production of photocatalysts at a good cost/benefit. That presents a high control of semiconductors' composition, morphology, and defect density. Thus, the development of new photocatalysts, in addition to considering their physical and chemical properties, must consider their availability or abundance, cost of production, and whether they are environmentally friendly.

Acknowledgments The authors are grateful to the National Council for Scientific and Technological Development (CNPq) Grants 573636/2008-7, 435975/2018-8, 309711/2019-3, and 421648/2018-0), Minas Gerais Research Funding Foundation (FAPEMIG) (Grant APQ-02075-21), Federal University of Ouro Preto-UFOP (Grant 23109.000928/2020-33), and São Paulo Research Foundation (Grant 2018/12871-0, 2012/07067-0, 2013/23572-0, 2016/019405, and 2013/07296). Special thanks are due to CEPID (2013/07296-2) and INCTMN (2008/57872-1). This study was financed in part by the Coordination for the Improvement of Higher Education Personnel (CAPES – Brazil) – Finance Code 001, CAPES-EPIDEMIAS (Programa Estratégico Emergencial de Prevenção e Combate a Surtos, Endemias, Epidemias e Pandemias Número do Processo: 88887.513223/2020-00).

References

M. Aggarwal et al., Photocatalytic carbon dioxide reduction: Exploring the role of ultrathin 2D graphitic carbon nitride (g-C3N4). Chem. Eng. J. **425**, 131402–131417 (2021). https://doi.org/10.1016/j.cej.2021.131402

X. Chang, T. Wang, J. Gong, CO2 photo-reduction: Insights into CO2 activation and reaction on surfaces of photocatalysts. Energy Environ. Sci. **9**, 2177–2196 (2016). https://doi.org/10.1039/C6EE00383D

R. Chong et al., Hydroxyapatite decorated TiO2 as efficient photocatalyst for selective reduction of CO2 with H2O into CH4. Int. J. Hydrog. Energy **43**, 22329–22339 (2018). https://doi.org/10.1016/j.ijhydene.2018.10.045

A. Crake et al., Titanium dioxide/carbon nitride nanosheet nanocomposites for gas phase CO2 photoreduction under UV-visible irradiation. Appl. Catal. B Environ. **242**, 369–378 (2019). https://doi.org/10.1016/j.apcatb.2018.10.023

M. Crippa et al., Fossil CO2 and GHG emissions of all world countries – 2019 Report, EUR 29849 EN. Available at: https://op.europa.eu/en/publication-detail/-/publication/9d09ccd1-e0dd-11e9-9c4e-01aa75ed71a1/language-en. Accessed 04 January 2022 (2019)

S. Diallo-Garcia et al., Identification of surface basic sites and acid–base pairs of hydroxyapatite. J. Phys. Chem. C **118**, 12744–12757 (2014). https://doi.org/10.1021/jp500469x

J. Ding et al., Micro-structured Cu-ZSM-5 catalyst on aluminum microfibers for selective catalytic reduction of NO by ammonia. Catalysis Today. Elsevier B.V. https://doi.org/10.1016/j.cattod.2021.05.013 (2021)

N.Y. Dzade, CO2 and H2O coadsorption and reaction on the low-index surfaces of tantalum nitride: A first-principles DFT-D3 investigation. Catalysts **10**, 1217–1231 (2020). https://doi.org/10.3390/catal10101217

D. Gielen, F. Boshell, D. Saygin, Climate and energy challenges for materials science. Nat. Mater. **15**, 117–120 (2016). https://doi.org/10.1038/nmat4545

L.F. Gorup et al., Chapter 2 – Methods for design and fabrication of nanosensors: The case of ZnO-based nanosensor, in *Micro and Nano Technologies*, ed. by B. Han et al., (Elsevier, 2020), pp. 9–30. https://doi.org/10.1016/B978-0-12-819870-4.00002-5

E. Grol, A. Zoelle, G.H. McIlvried, Enthalpy and free energy of CO2 utilization pathways (National Energy Technology Laboratory, 2017). Available at: https://www.osti.gov/biblio/1608105-enthalpy-free-energy-co2-utilization-pathways (2017)

A.D. Handoko, J. Tang, Controllable proton and CO2 photoreduction over Cu2O with various morphologies. Int. J. Hydrog. Energy **38**, 13017–13022 (2013). https://doi.org/10.1016/j.ijhydene.2013.03.128

I.M. Hegazy et al., Influence of oxygen vacancies on the performance of ZnO nanoparticles towards CO2 photoreduction in different aqueous solutions. J. Environ. Chem. Eng. **8**, 103887–103895 (2020). https://doi.org/10.1016/j.jece.2020.103887

T. Inoue et al., Photoelectrocatalytic reduction of carbon dioxide in aqueous suspensions of semiconductor powders. Nature **277**, 637–638 (1979). https://doi.org/10.1038/277637a0

N. de Jesus Martins et al., Facile preparation of ZnO:g-C3N4 heterostructures and their application in amiloride photodegradation and CO2 photoreduction. J. Alloys Compd. **856**, 156798–156805 (2021). https://doi.org/10.1016/j.jallcom.2020.156798

Q. Jin, M.F. Kirk, Thermodynamic and kinetic response of microbial reactions to high CO2. Frontiers in Microbiology. Qusheng Jin, Department of Earth Sciences, University of Oregon, Eugene, OR, USA, qjin@uoregon.edu, 7, pp. 1696–1716. https://doi.org/10.3389/fmicb.2016.01696 (2016)

A.D.N. Kamkeng et al., Transformation technologies for CO2 utilisation: Current status, challenges and future prospects. Chem. Eng. J. **409**, 128138–128168 (2021). https://doi.org/10.1016/j.cej.2020.128138

P. Kar et al., High rate CO2 photoreduction using flame annealed TiO2 nanotubes. Appl. Catal. B Environ. **243**, 522–536 (2019). https://doi.org/10.1016/j.apcatb.2018.08.002

N. Karachi et al., Novel high performance reduced graphene oxide based nanocatalyst decorated with Rh2O3/Rh-NPs for CO2 photoreduction. J. Photochem. Photobiol. A Chem. **364**, 344–354 (2018). https://doi.org/10.1016/j.jphotochem.2018.06.024

R. Kortlever et al., Catalysts and reaction pathways for the electrochemical reduction of carbon dioxide. J. Phys. Chem. Lett. **6**, 4073–4082 (2015). https://doi.org/10.1021/acs.jpclett.5b01559

V. Kumaravel, J. Bartlett, S.C. Pillai, Photoelectrochemical conversion of carbon dioxide (CO2) into fuels and value-added products. ACS Energy Lett. **5**, 486–519 (2020). https://doi.org/10.1021/acsenergylett.9b02585

H. Li et al., Improved photocatalytic activity of ZnO via the modification of In2O3 and MoS2 surface species for the photoreduction of CO2. Appl. Surf. Sci. **566–575**, 150649 (2021). https://doi.org/10.1016/j.apsusc.2021.150649

P. Li et al., Crystal facet-dependent CO2 photoreduction over porous ZnO nanocatalysts. ACS Appl. Mater. Interfaces **12**, 56039–56048 (2020). https://doi.org/10.1021/acsami.0c17596

L. Liang et al., Infrared light-driven CO2 overall splitting at room temperature. Joule **2**, 1004–1016 (2018). https://doi.org/10.1016/j.joule.2018.02.019

S.-H. Liu et al., Enhanced photoreduction of CO2 into methanol by facet-dependent Cu2O/reduce graphene oxide. J. CO2 Util. **33**, 171–178 (2019). https://doi.org/10.1016/j.jcou.2019.05.020

Z. Liu et al., Thermodynamic and kinetics of hydrogen photoproduction enhancement by concentrated sunlight with CO2 photoreduction by heterojunction photocatalysts. Energy AI **6**, 100102–100108 (2021). https://doi.org/10.1016/j.egyai.2021.100102

J. Mao, K. Li, T. Peng, Recent advances in the photocatalytic CO2 reduction over semiconductors. Cat. Sci. Technol. **3**, 2481–2498 (2013). https://doi.org/10.1039/C3CY00345K

S. Navarro-Jaén et al., Highlights and challenges in the selective reduction of carbon dioxide to methanol. Nat. Rev. Chem. **5**, 564–579 (2021). https://doi.org/10.1038/s41570-021-00289-y

Ș. Neațu, J.A. Maciá-Agulló, H. Garcia, Solar light photocatalytic CO2 reduction: General considerations and selected bench-mark photocatalysts. Int. J. Mol. Sci. **15**, 5246–5262 (2014). https://doi.org/10.3390/ijms15045246

A.E. Nogueira et al., New approach of the oxidant peroxo method (OPM) route to obtain Ti(OH) 4 nanoparticles with high photocatalytic activity under visible radiation. Int. J. Photoenergy. Hindawi Limited (2018). https://doi.org/10.1155/2018/6098302

A.E. Nogueira et al., Insights into the role of CuO in the CO2 photoreduction process. Sci. Rep. **9**, 1316–1326 (2019). https://doi.org/10.1038/s41598-018-36683-8

A.E. Nogueira, G.T.S.T. Silva, et al., CuO decoration controls Nb2O5 photocatalyst selectivity in CO2 reduction. ACS Appl. Energy Mater. **3**, 7629–7636 (2020a). https://doi.org/10.1021/acsaem.0c01047

A.E. Nogueira, G.T.S.T. da Silva, et al., Unveiling CuO role in CO2 photoreduction process – Catalyst or reactant? Catal. Commun. **137**, 105929–105933 (2020b). https://doi.org/10.1016/j.catcom.2020.105929

B. Ohtani, Photocatalysis A to Z—What we know and what we do not know in a scientific sense. J Photochem Photobiol C: Photochem Rev **11**, 157–178 (2010). https://doi.org/10.1016/j.jphotochemrev.2011.02.001

J.A. Oliveira et al., Photocatalytic CO2 reduction over Nb2O5/basic bismuth nitrate nanocomposites. Mater. Res. Bull. **133**, 111073–111083 (2021). https://doi.org/10.1016/j.materresbull.2020.111073

J.O. Olowoyo et al., Self-assembled reduced graphene oxide-TiO2 nanocomposites: Synthesis, DFTB+ calculations, and enhanced photocatalytic reduction of CO2 to methanol. Carbon **147**, 385–397 (2019). https://doi.org/10.1016/j.carbon.2019.03.019

Y. Qin et al., Highly efficient and selective photoreduction of CO2 to CO with nanosheet g-C3N4 as compared with its bulk counterpart. Environ. Res. **195**, 110880–110887 (2021). https://doi.org/10.1016/j.envres.2021.110880

L.S. Ribeiro et al., Rapid microwave-assisted hydrothermal synthesis of CuBi2O4 and its application for the artificial photosynthesis. Mater. Lett. **275**, 128165–128168 (2020). https://doi.org/10.1016/j.matlet.2020.128165

Y. Sakhno et al., Surface hydration and cationic sites of nanohydroxyapatites with amorphous or crystalline surfaces: A comparative study. J. Phys. Chem. C **114**, 16640–16648 (2010). https://doi.org/10.1021/jp105971s

G.T.S.T. da Silva et al., Acidic surface niobium pentoxide is catalytic active for CO2 photoreduction. Appl. Catal. B Environ. **242**, 349–357 (2019). https://doi.org/10.1016/j.apcatb.2018.10.017

G.T.S.T. da Silva et al., Redução de CO2 em hidrocarbonetos e oxigenados: Fundamentos, estratégias e desafios. Química Nova **44**, 963–981 (2021)

C. Song, CO_2 conversion and utilization: An overview, in *CO_2 conversion and utilization*, (American Chemical Society (ACS Symposium Series), 2002), pp. 1–2. https://doi.org/10.1021/bk-2002-0809.ch001

Z. Sun et al., Fundamentals and challenges of electrochemical CO2 reduction using two-dimensional materials. Chem **3**, 560–587 (2017). https://doi.org/10.1016/j.chempr.2017.09.009

J.A. Torres et al., Enhancing TiO2 activity for CO2 photoreduction through MgO decoration. J. CO2 Util. **35**, 106–114 (2020). https://doi.org/10.1016/j.jcou.2019.09.008

U. Ulmer et al., Fundamentals and applications of photocatalytic CO2 methanation. Nat. Commun. **10**, 3169–3180 (2019). https://doi.org/10.1038/s41467-019-10996-2

Q. Wang, K. Domen, Particulate Photocatalysts for light-driven water splitting: Mechanisms, challenges, and design strategies. Chem. Rev. **120**, 919–985 (2020). https://doi.org/10.1021/acs.chemrev.9b00201

J.L. White et al., Light-driven heterogeneous reduction of carbon dioxide: Photocatalysts and photoelectrodes. Chem. Rev. **115**, 12888–12935 (2015). https://doi.org/10.1021/acs.chemrev.5b00370

D. Wu et al., Green synthesis of boron and nitrogen co-doped TiO2 with rich B-N motifs as Lewis acid-base couples for the effective artificial CO2 photoreduction under simulated sunlight. J. Colloid Interface Sci. **585**, 95–107 (2021). https://doi.org/10.1016/j.jcis.2020.11.075

S. Xie et al., Photocatalytic and photoelectrocatalytic reduction of CO2 using heterogeneous catalysts with controlled nanostructures. Chem. Commun. **52**, 35–59 (2016). https://doi.org/10.1039/C5CC07613G

N. Zhang et al., Recent progress on advanced design for photoelectrochemical reduction of CO2 to fuels. Sci. China Mater. **61**(6), 771–805 (2018). https://doi.org/10.1007/s40843-017-9151-y

Z. Zhu et al., Preparation of Pd–Au/TiO2–WO3 to enhance photoreduction of CO2 to CH4 and CO. J. CO2 Util. **28**, 247–254 (2018). https://doi.org/10.1016/j.jcou.2018.10.006